

Snow depth distribution and wind processes of high mountain Central Chile: A new experimental setup

Thomas E. Shaw¹, Pablo Mendoza^{1,2}, Christian Oberli³, James McPhee^{1,2}

¹ Advanced Mining Technology Center, Universidad de Chile, Santiago, Chile

² Department of Civil Engineering, Universidad de Chile, Santiago, Chile

³ Escuela de Ingeniería Pontificia Universidad Católica de Chile, Chile



UNIVERSIDAD DE CHILE



1. Background

The quantity of water storage in the Chilean Andes is highly important for industry, agriculture and water supply to the region (approximately 40% of Chile's population live in Santiago), though remains poorly understood. Lack of high elevation in situ observations, combined with the complex topography of the Andes range, make predictions about the spatial and temporal variability of snow water equivalent difficult.

A particular uncertainty is associated with the preferential deposition and re-distribution of snow during storm events (Freudiger et al., 2017), which may be amplified by the generally dry conditions of the region (Li and Pomeroy, 1997). Here we present a newly established experimental catchment with the purpose of understanding local effects of wind on spatial snow depth distribution.

2. Study site

The upper headwalls of the Valle Nevado basin known as Piuquenes (33.31°S, 70.52°W) is a mostly unvegetated catchment of ~1.9 km² (Figure 1). The site lies between 3500 and 3800 m a.s.l. at the upper most reach of the La Parva ski resort, located almost 40 km east of the centre of Santiago, Chile (Figure 2). Central Chile is classified by a mediterranean climate, and the high elevation Andes range act as an important storage of snow for the seasonally dependent precipitation in the region (Meza et al., 2012). The data/experimental setup shown is for the 2018 season between June and September.

3. LiDAR

We employ a long range Reigl VZ-6000 LiDAR (Light Detection and Ranging) instrument to generate three-dimensional point clouds with an instrument angular resolution of 0.01° (~0.15 m @ 1.2 km range). The point clouds are registered using Reigl's RiScan software, georeferenced using differential GPS positions and rasterised to form a digital elevation model (DEM) of 0.5 m horizontal resolution. The subtraction of a base DEM without snow (obtained in January, 2018) from snow covered DEMs form the distributed snow depth maps throughout the winter season (Figure 3).

The point clouds are registered manually onto the base DEM acquisition using snow free bedrock and afterwards are registered with an automated cloud to cloud registration of the same snow free areas resulting in an error of ~0.04 m.



Figure 1: Image of basin and Position of LiDAR from January 2018

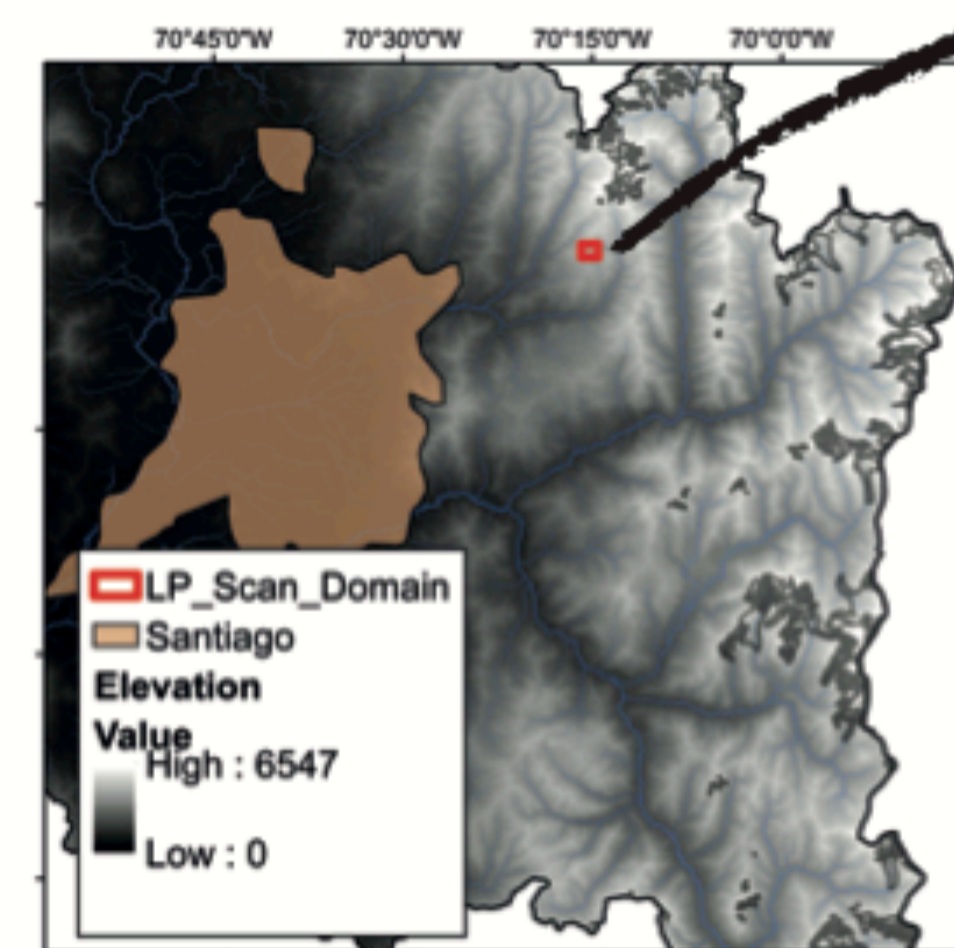


Figure 2: Map of the Metropolitan Region, and location of the basin relative to Santiago

5. Storm events of the 2018 Winter season

Figure 5 shows the principal storm events recorded at a low (Santiago) and medium elevation (mountain environment) station and the scan periods of the LiDAR (vertical green bars). A subset of the data highlights the high detail of information that is attainable from the LiDAR scanner that may be compared with in situ where data overlap exists.

2018 was a dry winter season in comparison with a 1980-2010 baseline, consistent with many of the years since 2010, characterising a 'mega-drought' (Garreaud et al., 2017). Maximum snow depths measured with the LiDAR were found during the field visits in August (Figure 5b-c). Evidence of wind re-distribution is seen between the weekly scans of 2nd and 9th August near node PQN6 (Figure 5b). The 2018 snow season for proximal ski resorts ended in early September, followed by recent (October) precipitation events (not captured by LiDAR acquisitions).

Interestingly, the quantity of precipitation recorded between stations on the west side of the study site is not a suitable proxy for snow depth measured between periods due to the origin of storms and local interaction of topography.

The mean, standard deviations and 90th percentile snow depths recorded were:

Date	Mean	Standard Deviation	90th Percentile
6 th June	0.28 m	0.23 m	0.56 m
26 th July	0.68 m	0.38 m	1.33 m
2 nd August	0.69 m	0.20 m	1.37 m
9 th August	0.88 m	0.53 m	1.59 m
28 th August	0.89 m	0.29 m	1.92 m
14 th September:	0.59 m	0.37 m	0.97 m

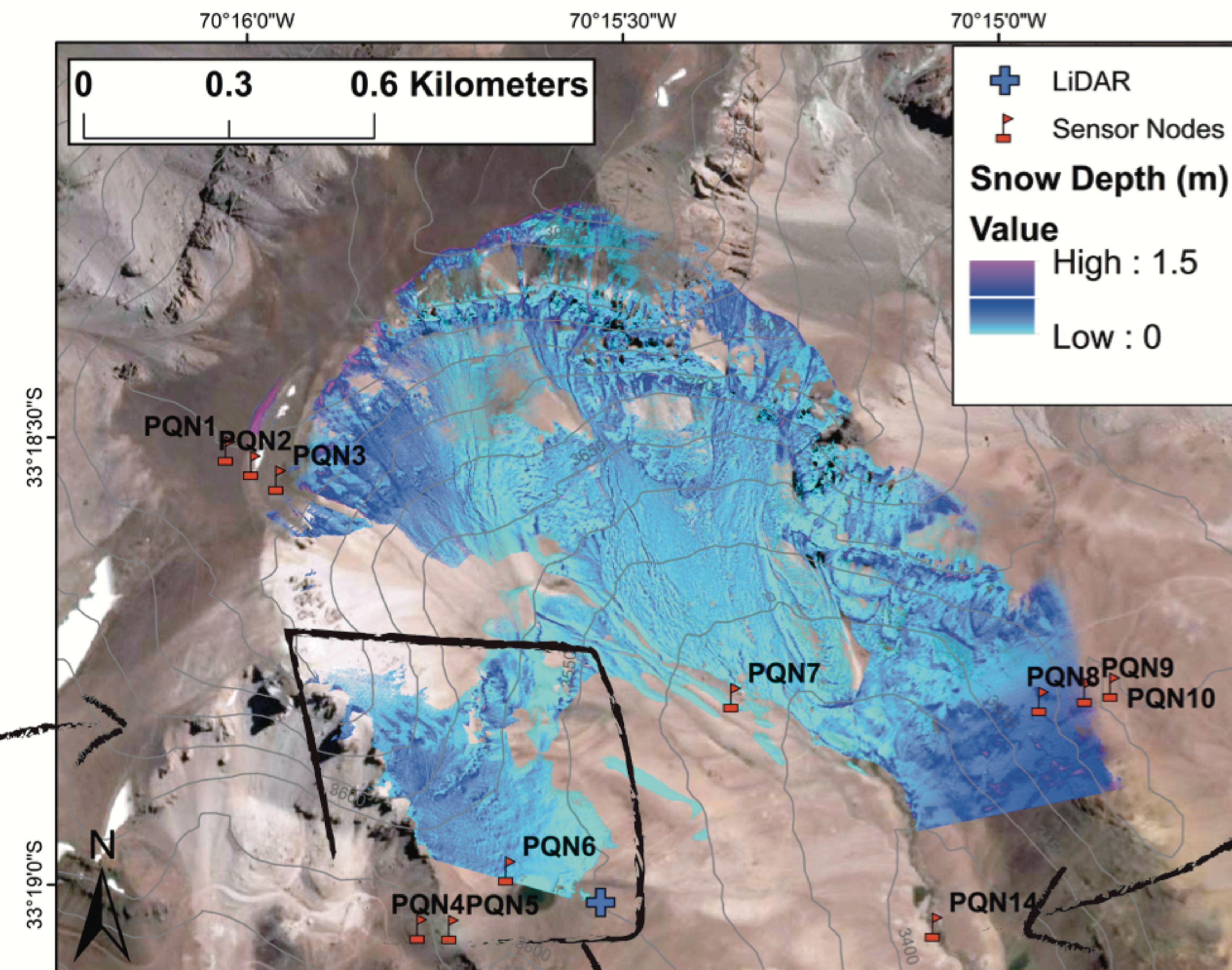


Figure 3: A map of the basin with LiDAR derived snow depth distribution for 2nd June, 2018. The locations of the 11 weather stations of the wireless network and LiDAR are shown.

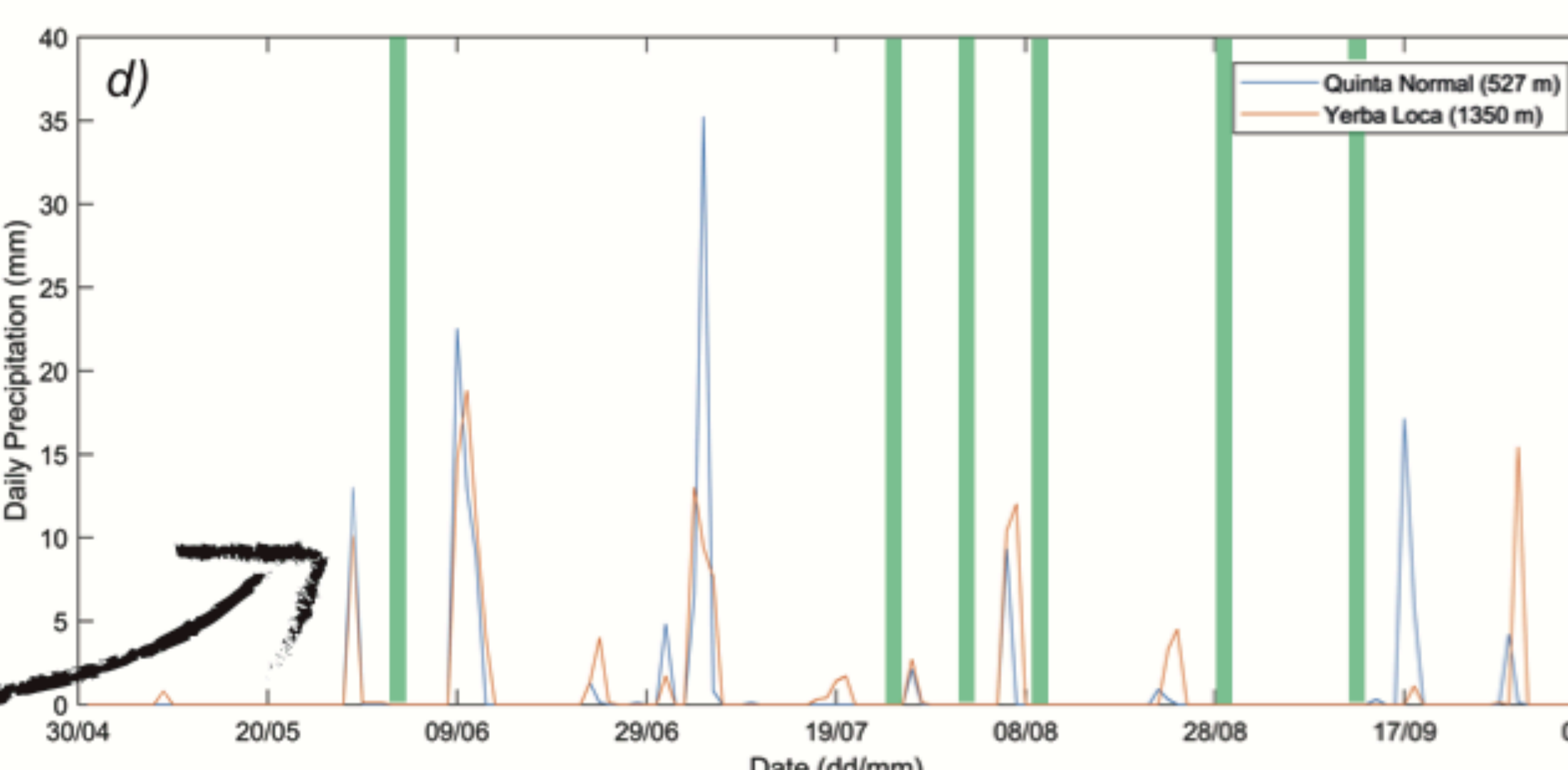
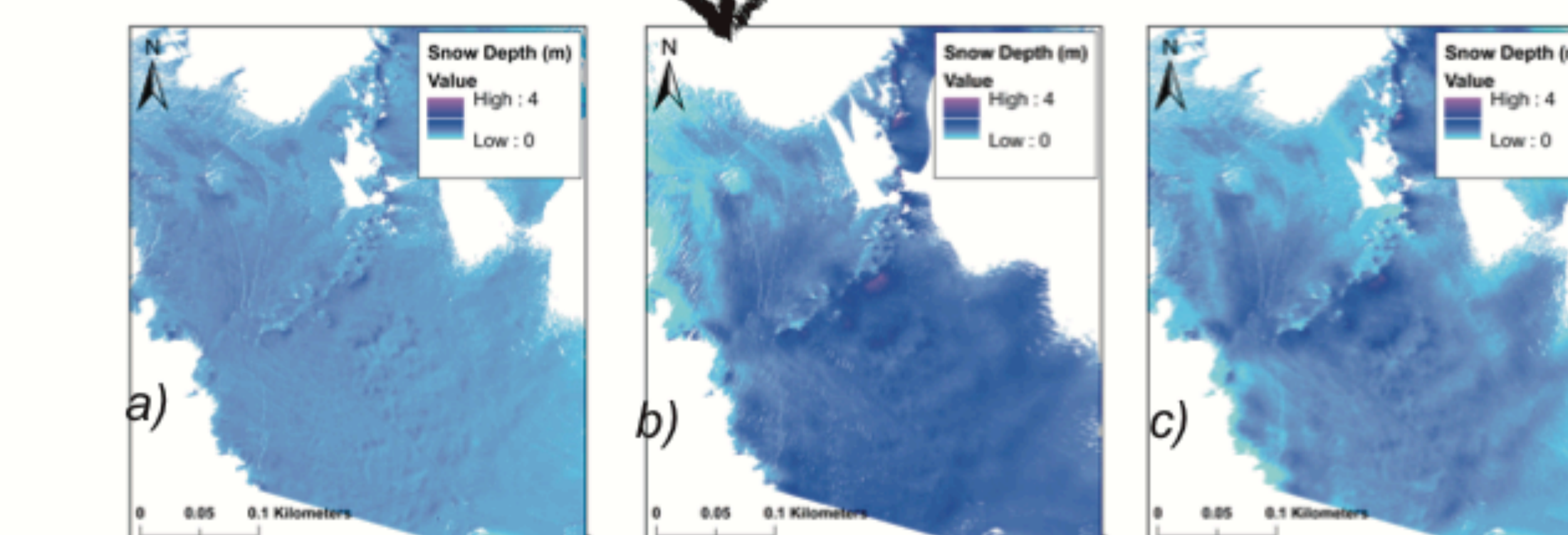


Figure 5: A local view of LiDAR snow depth distribution for a) 2nd June, b) 9th August and c) 28th August. Panel d) shows the scan periods relative to storm events recorded at two permanent stations (Source: DGA)

4. Wireless Sensor Network

A new series of wirelessly networked automatic weather stations (Latina UC) were installed within the basin in order to observe hourly variations in snow depth at three key transects related to the distribution of wind (PQN1-3,4-6 and 8-10, Figure 3). This is supplemented by two additional sensors, PQN7 and PQN14, the latter of which has a setup for monitoring streamflow from the basin (Figure 4).

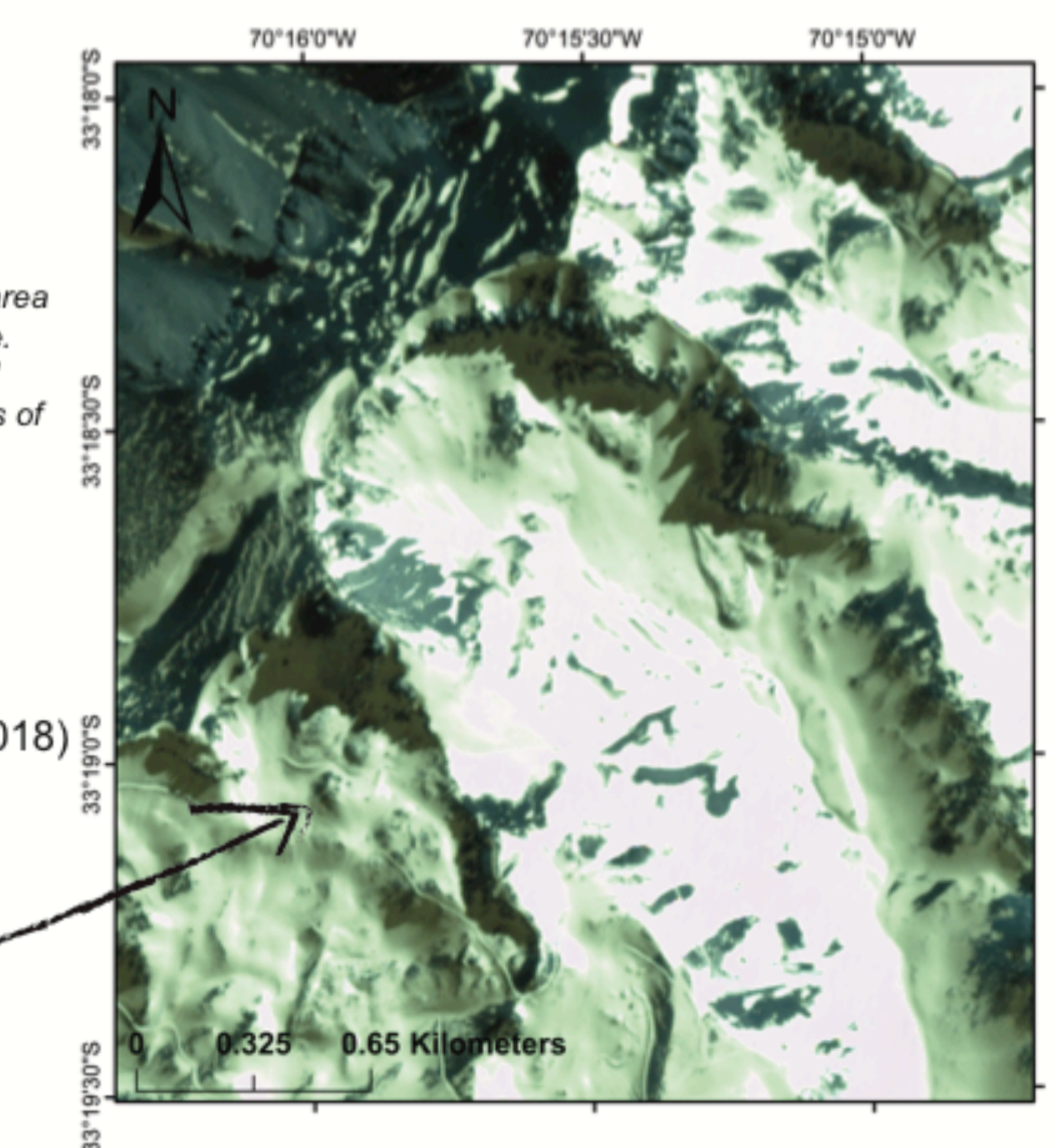
- Sensors are wirelessly networked and send 60 minute readings of meteorological variables and sonic snow depth to station PQN4 which sends the signal to Santiago.



Variable	Unit	Sites	Sampling period
Air temperature	°C	All	60 minutes
Relative air humidity	%	All	60 minutes
Wind speed	m/s	2, 5, 9, 14	60 minutes
Wind direction	°	2, 5, 9, 14	60 minutes
Gust speed	m/s	2, 5, 9, 14	60 minutes
Water temperature	°C	14	15 minutes
Electric conductivity of water	uS/cm	14	15 minutes
Water depth (hydrostatic)	cm	14	15 minutes
Atmospheric pressure	kPa	2, 5, 9, 14	60 minutes
Snow depth (ultrasonic)	cm	All	60 minutes

Figure 4 (left): Example of wireless sensor network station (PQN14)

Figure 6 (right): An example of snow cover area visible from a PlanetScope 3m optical image. Easily visible in the image is the melting and removal of snow on the north and west sides of the basin.



6. Satellite observations

- PlanetScope optical satellite images (Planet Team, 2018)

- 3 m horizontal resolution - daily revisit (Figure 5)

- To observe changes in snow covered area

- Validate LiDAR scans of zero snow

7. Future plans

- To identify the effect of key storm events on the spatial distribution of snow depth in the basin and its relationship to local topography

- To identify how well point measurements (Nodes) can represent changes of snow depth at the basin scale.

- To model wind re-distribution of snow using physically based models (DBSM - Essery et al., 1999), calibrated/validated with:

- > In situ observations
- > LiDAR scans at discrete time steps
- > Optical/thermal satellite products of high resolution (e.g. PlanetScope, Figure 6)
- > Relation of snow depth to regional climate and low elevation information
- > Sensitivity of region to future climate changes

References
 Essery, R., Li, L., and Pomeroy, J. (1999) 'A distributed model of blowing snow over complex terrain', *Hydrological Processes*, 13(14-15), pp. 2423-2438. doi: 10.1002/(SICI)1099-1085(199910)13:14<2423::AID-HYP853>3.0.CO;2-U.
 Freudiger, D. et al. (2017) 'Snow redistribution for the hydrological modeling of alpine catchments', *Water*, 9, #1232. doi: 10.1002/wat2.1232.
 Garreaud, R. et al. (2017) 'The 2010-2015 mega drought in Central Chile: Impacts on regional hydroclimate and vegetation', *Hydrology and Earth System Sciences* pp. 1-37. doi: 10.5194/hess-2017-191.
 Li, L. and Pomeroy, J. (1997) 'Probability of occurrence of blowing snow', *Journal of Geophysical Research*, 102(D18), 21955-21964.
 Meza, F. J., et al. (2012) 'Impacts of Climate Change on Irrigated Agriculture in the Maipo Basin, Chile - Reliability of Water Rights and Changes in the Demand for Irrigation', pp. 421-430. doi: 10.1061/(ASCE)WR.1943-5452.